

# Epidemiologically and Socio-economically Optimal Policies via Bayesian Optimization

Amit Chandak      Debojyoti Dey      Bhaskar Mukhoty  
 Purushottam Kar  
 Indian Institute of Technology Kanpur  
 {amitch,debojyot,bhaskarm,purushot}@cse.iitk.ac.in

April 26, 2020

## Abstract

Mass public quarantining, colloquially known as a *lock-down*, is a non-pharmaceutical intervention to check spread of disease. We present **ESOP**, a novel application of active machine learning techniques using Bayesian optimization, that interacts with an epidemiological model to arrive at lock-down schedules that optimally balance public health benefits and socio-economic downsides of reduced economic activity during lock-down periods. The utility of **ESOP** is demonstrated using case studies with **VIPER**, a stochastic agent-based simulator that we also propose. However, **ESOP** can flexibly interact with arbitrary epidemiological simulators and produce schedules that involve multiple phases of lock-downs.

**Disclaimer:** *This document makes no recommendation to individuals. Results presented herein should not be interpreted to modulate personal behavior. The authors strongly recommend that individuals continue to follow guidelines offered by local governments with respect to lock-downs and social distancing and those offered by medical professionals with respect to personal hygiene and treatment.*

## 1 Introduction

Infectious diseases that are contagious pose a threat to public safety once they attain pandemic status. Several historical instances of such pandemics have taken a heavy toll on human lives. Prominent examples include the H1N1 (Spanish flu) pandemic of 1918 ( $> 50$  million fatalities), the H3N2 (HongKong flu) pandemic of 1968 ( $\approx 1$  million fatalities), the HIV/AIDS pandemic ( $\approx 32$  million fatalities) [Kimball and Bose, 2020], the novel influenza A H1N1 (swine flu) pandemic of 2009 ( $\approx 0.3$  million fatalities) [Roos, 2012], and the ongoing CoViD-19 pandemic ( $> 0.15$  million fatalities as of writing this document) [WHO, 2020].

In such situations, and especially in the absence of vaccines and antiviral treatments, experts often prescribe guidelines to public such as hand hygiene and respiratory etiquette, as well as two kinds of non-pharmaceutical interventions, namely 1) *mitigation policies* such as human surveillance and contact tracing, and 2) *suppression policies* such as social distancing or its more extreme form colloquially known as a *lock-down* [Aledort et al., 2007]. However, their benefits with respect to public health outcomes notwithstanding, severe and extended applications of suppression policies such as lock-downs negatively impact livelihoods and the economy. For instance, Scherbina [2020] estimates the cost of extensive suppression measures to the US economy at \$9 trillion, or about 43% of its annual GDP.

Moreover, Peak et al. [2017] demonstrate the need for policy decisions to balance suppression and mitigation measures in terms of the epidemiological characteristics of the pandemic, pointing out that suppression measures hold most benefit for fast-course diseases whereas effective mitigation measures may suffice for others at much less socio-economic cost. This points to a need for techniques that can take the disease progression characteristics of a certain outbreak and suggest policies that optimally use suppression and mitigation techniques to offer acceptable health outcomes as well as socio-economic risks within acceptable limits.

## 1.1 Related Works

Several works exist on modelling epidemic and pandemic progressions using differential equation-based models such as SIR or SEIR and using them to make predictions. Some examples include [Efimov and Ushirobira, 2020, Lyra et al., 2020, Sardar et al., 2020, Vyasarayani and Chatterjee, 2020]. Most of these studies utilize differential equation-based models such as SIR and SEIR variants. In this paper, we will instead use a stochastic agent-based model called VIPER which we propose and describe in Sec 2.

Micro-simulation studies using UK [Ferguson et al., 2020] and Indian [Singh and Adhikari, 2020] data conclude that multiple short-term suppression rounds may offer acceptable health outcomes when a single extended period of suppression is infeasible. However, these works do not offer ways to find either the optimal moment to initiate suppression measures or their duration.

This is important since Morris et al. [2020], Patterson-Lomba [2020] show that the optimal initiation point and duration depend on the disease characteristics themselves. This is understandable since premature suppression slows the depletion of the pool of susceptible individuals leaving room open for a second wave of infections whereas delayed suppression may cause the initial wave to be widespread in itself. Scherbina [2020] additionally considers the economic impact of these measures and suggests durations for lock-down periods and their associated economic costs in medical expenses as well as lost value of statistical life.

Prior works offering actual policy advice fall into two categories: 1) those that offer only broad principles on how to target interventions e.g. by identifying simple rules of thumb [Wallinga et al., 2010], and 2) those that do offer actionable advice e.g. when to initiate suppression [Morris et al., 2020]. However, the latter do not take the socio-economic impact of these measures into account and moreover, consider only simple theoretical models e.g. SIR that are not very expressive.

## 1.2 Our Contributions

We present ESOP, a system that uses Bayesian optimization to automatically suggest suppression policies that optimally balance public health and economic outcomes<sup>1</sup>. ESOP interacts with epidemiological models to automatically suggest policy decisions. We also present VIPER, an iterative, stochastic agent-based model (ABM) with which we conduct case studies to showcase the utility of ESOP. We note however, that ESOP can readily interact with other epidemiological models, e.g. those that incorporate stratification based on region and age e.g. INDSCI-SIM [Shekatkar et al., 2020], IndiaSim [Megiddo et al., 2014]. Although machine learning techniques have been used in epidemiological forecasting [Lindström et al., 2015] and estimating model parameters [Dandekar and Barbastathis, 2020], we are not aware of prior work using machine learning in epidemiological policy design.

# 2 VIPER: An Iterative Stochastic Agent-based Epidemiological Model

VIPER (Virus-Individual-Policy-EnviRonment) models an *in-silico* population of individuals, supports compartments of the SEIR model [Keeling and Rohani, 2008], and allows travel and quarantining of individuals. Being an ABM rather than an ODE-based model, VIPER can model disease progression within each individual separately and thus, quarantine or expire individuals based on their stage of the disease, something that is difficult to do in ODE-based models. Stochastic ABMs allow diverse socio-medico-economic traits to be modeled at the individual level but cannot be easily represented by a concise system of ODEs. Thus, works such as [Morris et al., 2020] do not apply here.

Details of the VIPER model are described below and succinctly enumerated in Tab 1. VIPER consists four *sub-models*, one each devoted to modelling individuals, the virus, environment parameters and policy parameters.

---

<sup>1</sup>All code used for this study is available at the following GitHub Repository <https://github.com/purushottamkar/esop>

Attr	Description	Range	Def	Attr	Description	Range	Ini
<b>Viral Model</b>				<b>Individual Model</b>			
INC	incubation period	$\mathbb{N}$	3	SUS	susceptibility to infection	$[0, 1]$	rnd
BVL	base viral load	$[0, 1]$	0.05	RST	resistance to disease progression	$[0, 1]$	rnd
DPR	disease progression rate	$[0, 1]$	0.1	VLD	current viral load	$[0, 1]$	0.0
XTH	VLD threshold for expiry	$[0, 1]$	0.7	RLD	current recovery load	$[0, 1]$	0.0
BXP	expiry probability at XTH	$[0, 1]$	0.0	STA	current state	SEIRX	S
<b>Environment Model</b>				QRN	quarantine status	0 or 1	0
BCR	contact radius b/w individuals	$[0, 1]$	0.25	X, Y	current location	$[0, 1]^2$	rnd
BIP	prob. infection upon contact	$[0, 1]$	0.5	<b>Policy Model</b>			
BTR	prob. of an individual traveling	$[0, 1]$	0.01	QTH	VLD threshold for quarantine	$[0, 1]$	0.3
BTD	maximum travel distance	$[0, 1]$	1.0	BQP	quarantine probability at QTH	$[0, 1]$	0.0
INI	initial rate of infection	$[0, 1]$	0.01	$l(t)$	lock-down level at time $t$	$[0, 5]$	—

Table 1: Attributes in the VIPER model, valid ranges and default/initial values. The state of an individual can be S (susceptible), E (exposed), I (infectious), R (recovered) or X (expired). Individuals are initialized with random values for RST, SUS and their location within the 2-D box  $[0, 1]^2$ . Individuals progress from state  $S \rightarrow E \rightarrow I$ , can be quarantined while in state I and then move to either state R or X. The viral load (VLD) of an individual represents the extent of infection within their system. At the end of the incubation period (INC), an exposed individual always has a viral load of BVL. The virus attempts to increase this viral load according to the disease progression rate (DPR) whereas the individual resists this according to their resistance level (RST) by converting viral load to recovery load (RLD). Disease progression in every infected individual is governed by an SIR-like model with  $\frac{d \text{VLD}(t)}{dt} = -\text{RST} \cdot \text{VLD}(t) + \text{DPR} \cdot (1 - \text{VLD}(t) - \text{RLD}(t))$  and  $\frac{d \text{RLD}(t)}{dt} = \text{RST} \cdot \text{VLD}(t)$ . An infected individual whose VLD falls below BVL moves on to state R. An individual with VLD equal to QTH (resp. XTH) has a probability BQP (resp. BXP) of getting quarantined (resp. expired) at every time step  $t$ . These probability values increase linearly to 1 as VLD goes up. Note that this allows VIPER to model asymptomatic transmission since it allows individuals with low VLD levels (esp. below QTH) to avoid detection with high probability. The lock-down level is specified at every time instant  $t$  of the simulation. A lock-down level of  $l(t)$  causes BTD as well as BCR at time  $t$  to go down by a factor of  $\exp(-l(t))$ . Thus, at high lock-down levels, individuals are neither able to travel much, nor have contact with other individuals far off from their current location.

**Individual Model** : an individual is characterized by their susceptibility to infection (SUS), resistance to disease progression (RST), viral load (VLD), recovery load (RLD), current state (STA), quarantine status (QRN) and location (X,Y). SUS, RST, VLD, RLD, X and Y are real numbers between 0 and 1, QRN takes Boolean values whereas STA can be either S (susceptible), E (exposed), I (infectious), R (recovered) or X (removed/deceased).

**Viral Model** : the virus is characterized by its incubation period (INC), the base viral load in an individual at the end of the incubation period (BVL), the disease progression rate (DPR), the viral load over which an individual's chances of getting expired start increasing (XTH) and the base removal probability of an individual with viral load at XTH (BXP). BVL, DPR, XTH and BXP are real numbers between 0 and 1 whereas INC is a natural number.

**Environment Model** : the environmental factors are modeled using the typical contact radius between individuals (BCR), the probability that a contact between an infectious and susceptible individual will lead to a successful infection (BIP), the fraction of the population that travels at any time instant (BTR), the maximum distance to which they travel (BTD), and the fraction of population that is infected with the virus at start of the simulation (INI). All these values are represented as real numbers between 0 and 1.

**Policy Model** : the policy model comprises the viral load over which an individual's chances of getting quarantined start increasing (QTH) and the base quarantining probability of an individual with viral load at QTH (BQP). Both are real numbers between 0 and 1. Additionally, the policy prescribes a *lock-down* level which is a real number between 0 and 5 for each time instant of the simulation. A lock-down level of  $l$  causes BTD as well as BCR to go down by a factor of  $\exp(-l)$ . Thus, at a high lock-down level, individuals are neither able to travel much, nor interact with other individuals far off from their current location.

**Modelling disease-progression dynamics in VIPER** : The state of an individual in the VIPER model can be either S (susceptible), E (exposed), I (infectious), R (recovered) or X (expired). Individuals, upon getting infected, progress from state S to state E and further onto state I. Individuals can be quarantined while in state I and then move to either state R or X.

The viral load (VLD) of an individual represents the extent of infection within their system. At the end of the incubation period (INC), an exposed individual always has a “base” viral load of BVL. The virus attempts to increase this viral load according to the disease progression rate (DPR) whereas the individual resists this according to their resistance level (RST) by converting viral load to recovery load (RLD). Disease progression in every infected individual is governed by an SIR-like model with

$$\frac{d \text{VLD}(t)}{dt} = -\text{RST} \cdot \text{VLD}(t) + \text{DPR} \cdot (1 - \text{VLD}(t) - \text{RLD}(t))$$

and

$$\frac{d \text{RLD}(t)}{dt} = \text{RST} \cdot \text{VLD}(t)$$

Thus, VIPER allows individuals to experience disease progression, as well as associated effects like quarantining or expiry, in a completely individualized manner, something that is readily possible in agent-based models but much more difficult to express in terms of a compact set of differential equations.

An infected individual whose VLD falls below BVL moves on to state R, i.e. recovers. An individual with VLD equal to QTH (resp. XTH) has a probability BQP (resp. BXP) of getting quarantined (resp. expired). An individual with VLD greater than QTH has the following probability of getting quarantined

$$\mathbb{P}[\text{quarantine}] = \text{BQP} + (1 - \text{BQP}) \cdot \frac{\text{VLD} - \text{QTH}}{1 - \text{QTH}},$$

i.e. the probability of getting quarantined increases linearly to 1 as the individual's VLD goes up. At every time step  $t$ , a coin is tossed for all individuals with VLD greater than QTH which lands heads with this particular probability. If the coin does indeed land heads, the individual is deemed quarantined. Note that this allows VIPER to model asymptomatic transmission since it allows individuals with low VLD levels (esp. below QTH) to avoid detection with high probability but makes it difficult for those in advanced stages of the disease to avoid quarantine.

Similarly, an individual with VLD greater than XTH has the following probability of getting expired

$$\mathbb{P}[\text{expiry}] = \text{BXP} + (1 - \text{BXP}) \cdot \frac{\text{VLD} - \text{XTH}}{1 - \text{XTH}}.$$

At every time step, a coin is similarly tossed to decide on whether an individual with VLD greater than XTH gets expired or not. The lock-down level needs to be specified at every time instant  $t$  of the simulation. A lock-down level of  $l(t)$  causes BTD as well as BCR at that time  $t$  to go down by a factor of  $\exp(-l(t))$ . Thus, at high lock-down levels, individuals are neither able to travel much, nor have contact with other individuals far off from their current location. The lock-down level has no effect on the quarantining or expiry processes described above which continue the same way irrespective of the lock-down level.

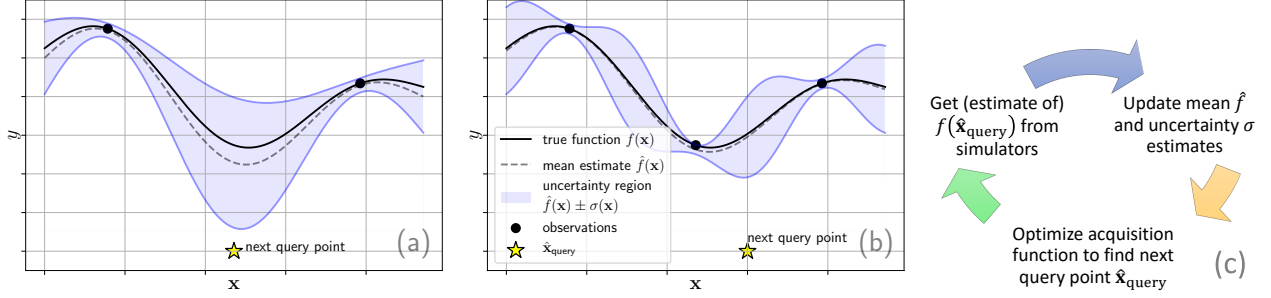


Figure 1: An illustration of the Bayesian optimization process. The algorithm uses the current observations and Gaussian process regression [Rasmussen and Williams, 2006] to obtain a *mean* estimate  $\hat{f}(\mathbf{x})$  (dashed line) of the true function  $f(\mathbf{x})$  (bold line) as well as an estimate  $\sigma(\mathbf{x})$  of the *uncertainty* in that estimate (the blue shaded region depicts  $\hat{f}(\mathbf{x}) \pm \sigma(\mathbf{x})$ ). Notice that uncertainty drops around observation points since (a good estimate of) the true function value is known there. Using these, an *acquisition* function is created. Fig 1(a) uses the simple LCB (lower confidence bound) acquisition function defined as  $a(\mathbf{x}) = \hat{f}(\mathbf{x}) - \sigma(\mathbf{x})$ . Other possibilities include EI (expected improvement) and KG (knowledge gradient). The (estimated) function value at the point  $\hat{\mathbf{x}}_{\text{query}} := \arg \min a(\mathbf{x})$  is now queried. Using  $f(\hat{\mathbf{x}}_{\text{query}})$ , the mean and uncertainty estimates  $\hat{f}, \sigma$  are updated as shown in Fig 1(b) and the process is repeated. At the end, the query point with the lowest function value is returned as the estimated minimum. Note that ESOP can only query VIPER but does not have access to its internal attribute values.

### 3 ESOP: Epidemiologically and Socio-economically Optimal Policies

We encode interventions as vectors and their health and socio-economic outcomes as functions, e.g., the coordinates of a 2-D vector  $\mathbf{x} = [\mathbf{x}_1, \mathbf{x}_2] \in \mathbb{N}^2$  may encode the starting point ( $\mathbf{x}_1$ ) and duration ( $\mathbf{x}_2$ ) of a lock-down. Next, consider a function  $f_{\text{epi}} : \mathbb{N}^2 \rightarrow [0, 1]$  encoding health outcomes with  $f_{\text{epi}}(\mathbf{x})$  equal to the peak infection rate (the largest fraction of the total population infected at any point of time) if the intervention  $\mathbf{x}$  is applied. Similarly, let  $f_{\text{eco}} : \mathbb{N}^2 \rightarrow [0, 1]$  encode economic outcomes with  $f_{\text{eco}}(\mathbf{x})$  being the fraction of population that would face unemployment if lock-down were indeed to last  $\mathbf{x}_2$  days. We stress that the functions  $f_{\text{epi}}, f_{\text{eco}}$  described here are examples and other measurable outcomes, e.g. cumulative death rate, loss to GDP, can also be used. Predicted estimates for  $f_{\text{epi}}$  would be obtained from epidemiological simulators such as INDSCI-SIM or IndiaSim (we will use VIPER) and those for  $f_{\text{eco}}$  would be obtained from economic models. Our goal is to balance health and economic outcomes by solving the following optimization problem:

$$\mathbf{x}^* := \arg \min_{\mathbf{x} \in \mathbb{N}^2} f(\mathbf{x}) \text{ where } f(\mathbf{x}) = f_{\text{epi}}(\mathbf{x}) + f_{\text{eco}}(\mathbf{x})$$

However, it is challenging to perform this optimization using standard descent techniques [Boyd and Vandenberghe, 2004] since even obtaining values of the function  $f$  at specific query points (let alone gradients) is expensive as it involves querying simulators such as VIPER. An acceptable solution in this case is Bayesian optimization [Jones et al., 1998] which is an *active machine learning* technique used to optimize functions which are expensive to evaluate and to which, moreover we do not have access to gradients. The technique adaptively queries the function at only a few locations to quickly approximate the solution to the optimization problem. Fig 1 outlines the basic steps in Bayesian optimization. Lack of space does not permit a detailed overview and we refer the reader to [Frazier, 2018] for an excellent review. ESOP additionally employs multi-scale search and caching techniques to accelerate computations.

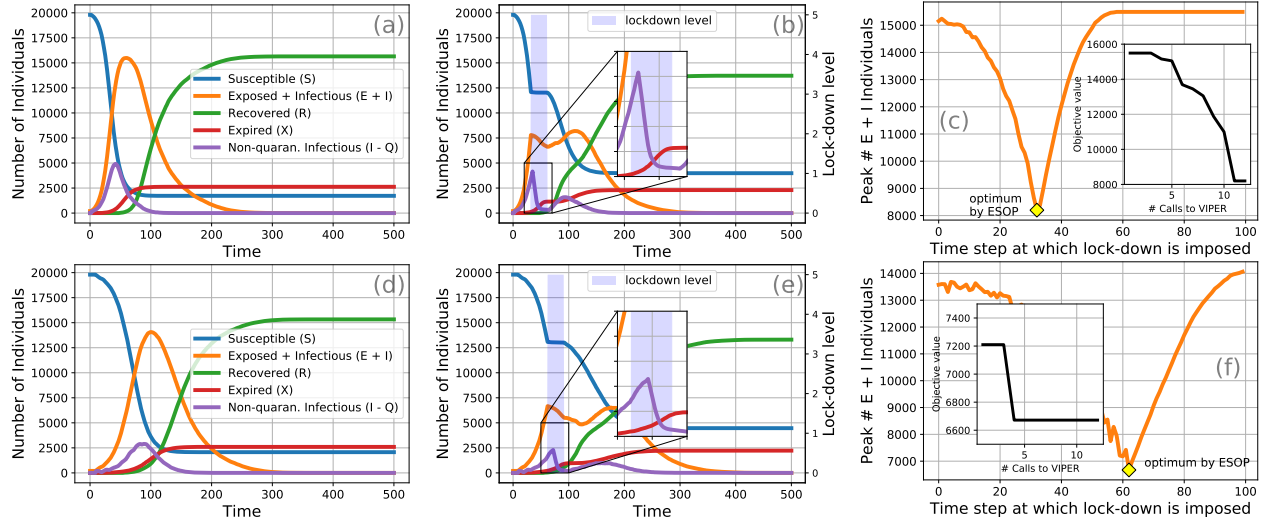


Figure 2: Fig 2(a) shows the daily number of individuals in various categories if no suppression is used. Note the large number of non-quarantined yet infectious individuals who are responsible for disease spread. The number of infected (E+I) individuals peaks at around 15500 at  $t = 58$ . For Fig 2(b), ESOP was asked to suggest when to start a 30 day lock-down at level 5. It suggested starting at  $t = 33$  with the peak reducing to 8200. Fig 2(c) shows that ESOP achieved the globally optimal initiation point within just 12 calls to VIPER (see inset figure). For Fig 2(c), VIPER was queried with all  $i \in [0, 100]$  to explicitly find the globally optimum. Fig 2(d-f) show the same results but for a viral strain that has an incubation of 10 days instead of 3 days. The optimal initiation point depends strongly on the incubation period of the virus but ESOP discovers it in both cases. Also note that the number of non-quarantined infectious individuals continues to rise (see Fig 2(b) and (e) insets) even after imposition of lock-down due to the incubation period of the disease (rise is longer if the incubation period is longer).

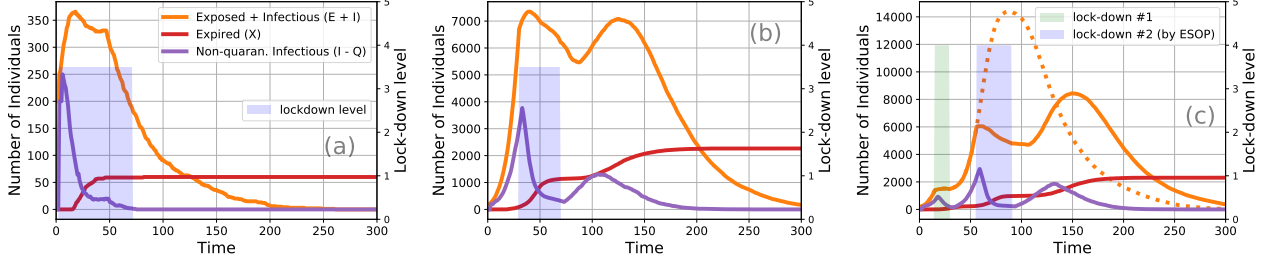


Figure 3: For Fig 3(a), ESOP was asked to suggest a lock-down (no constraints on duration etc). It suggested one at level 3.5 starting  $t = 3$ , lasting 69 steps, resulting in a peak of 303 infections (much smaller than the peaks in Fig 2) and 1092 predicted cases of unemployment.  $f_{eco}$  prevents the lock-down from going on indefinitely. The suggested lock-down seems to adopt a containment strategy, initiating a moderate-level suppression very early on to deplete the pool of infectious individuals. Note that the pool of non-quarantined infectious individuals is indeed exhausted by the time the suggested lock-down is over, preventing a second wave of infections. For Fig 3(b), ESOP was forced to suggest a lock-down starting no earlier than  $t = 12$  and no longer than 40 days. Since infections are already rampant by  $t = 12$ , ESOP adopts a mitigation strategy of starting a lock-down at  $t = 30$  for 40 steps at level 3.5, causing a peak of 7353 infections and 560 cases of unemployment. Notice that the lock-down is delayed strategically so that the second wave that comes thereafter does not have a higher peak, thus balancing the two peaks indeed as dictated by  $f_{epi}$ . For Fig 3(c), ESOP was given a situation where an earlier lock-down (green shading) had already taken place but was ineffective and left alone, would have caused a massive second wave with a peak of 14384 (dotted orange curve). ESOP suggests a second lock-down starting at  $t = 56$  lasting 35 steps at level 4 which brings the peak down to a much lower level of 8447 and causing 560 additional cases of unemployment.

## 4 Experimental Case Studies

We present case studies with VIPER simulating an in-silico population of 20000 individuals (ESOP readily scales to much larger populations as well). The default/initial settings of attributes in VIPER are given in Tab 1. Any modifications to these are mentioned below.

**Finding the optimal initiation point of a lock-down** : Fig 2 considers a simple case where we have decided to impose a 30 time step lock down at level 5 but are unsure when to initiate the lock down for optimal effect. The objective here is to minimize  $f_{epi}$  alone (i.e.  $f_{eco}$  is not considered). For any initiation point  $i \in \mathbb{N}$ , we let  $f_{epi}(i)$  be the largest number of individuals in E and I states at any given point of time – the so called *peak* of the curve – if a level 5 lock-down is initiated at  $t = i$ . The results show that the optimal initiation point depends significantly on the disease characteristics, in particular the incubation period of the virus. Nevertheless, ESOP always found a near-optimal solution in very few iterations offering far superior health outcomes compared to a no-lock-down scenario.

**Optimizing lock-downs under constraints** : Fig 3 considers finding the optimal initiation ( $i$ ), period ( $p$ ) and level ( $l$ ) of a lock-down, subject to constraints. A lock-down is represented as a 3-D vector  $\mathbf{x} = (i, p, l)$ . Our objective is to minimize  $f_{epi} + f_{eco}$  where  $f_{epi}(\mathbf{x})$  is the peak of the E+I curve and  $f_{eco}(\mathbf{x}) = \frac{l}{5} \cdot p \cdot \frac{N}{1000}$  estimates job losses due to the lock-down assuming a level- $l$  lock-down forces an  $\frac{l}{50}$  percent of the population of  $N = 20000$  into unemployment each day for  $p$  days (ESOP works for other definitions of  $f_{eco}$  too). Fig 3 shows (see caption) that ESOP is able to shift from a containment to a mitigation strategy depending on the constraints. Note that when multiple spikes are inevitable due to constraints on the lock-down (e.g. upper limits on the duration), ESOP always balances the heights of those spikes to ensure that infections are evenly distributed among them.

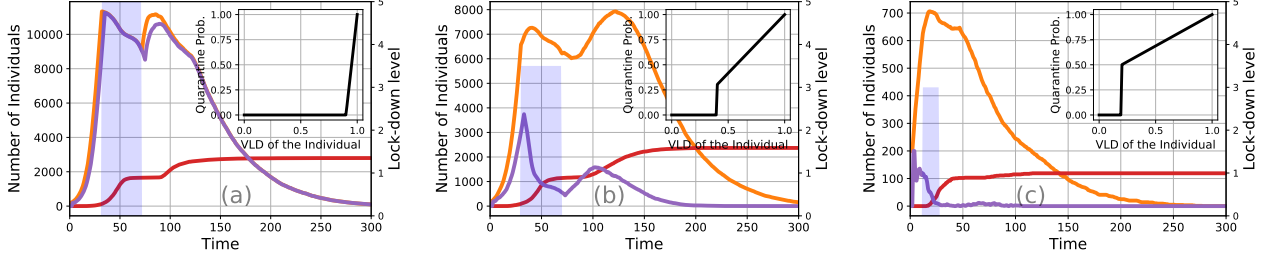


Figure 4: Fig 4(a) considers sluggish quarantining with  $QTH = 0.9$  and  $BQP = 0.0$  (the quarantining probability profile is shown in Fig 4(a) inset). Almost no individuals get quarantined here and despite its best efforts, ESOP is only able to offer 11338 peak infections and 800 unemployment cases using a lock-down starting at  $t = 32$  lasting 40 steps at level 5. The situation improves in Fig 4(b) with stronger quarantining at  $QTH = 0.4$  and  $BQP = 0.3$ . Here, ESOP offers fewer infections (7930) and job losses (560) using a lock-down at a reduced level of 3.5 (starting  $t = 30$  for 40 steps). The situation improves further in Fig 4(c) where we have even stronger quarantining at  $QTH = 0.2$  and  $BQP = 0.5$  with ESOP offering a peak of just 706 and 192 job losses using a lock-down of level 3 starting  $t = 12$  and lasting just 16 steps.

**Can aggressive quarantining permit less severe lock-downs?** : Fig 4 looks at the situation in Fig 3(b), but with varying quarantine aggressiveness. As Tab 1 explains, individuals with viral loads over a threshold  $QTH$  get quarantined with a probability profile. Using greater screening and public awareness, this profile can be altered. Fig 4 shows the health and economic benefits of the same.

## 5 Concluding Remarks

Incorporating age stratification and climate into VIPER and augmenting ESOP to suggest age- and climate-specific policies would be interesting. Being non-linear systems with negative feedback loops, epidemiological models may exhibit chaotic behavior [Bolker, 1993, Eilersen et al., 2020]. It is interesting to study how techniques like ESOP can be adapted to such settings.

### 5.1 Relevance to CoViD-19 and Future Prospects

Given the evolving nature of the current CoViD-19 pandemic, a technique like ESOP helps in optimally designing multi-phase lock-downs, thus avoiding speculation and human error. As shown in Sec 4, whenever multiple waves of infection are unavoidable due to constraints on lock-downs, ESOP offers lock-down schedules that balance the peaks of these multiple outbreaks, ensuring no peak is too high. To maximize the impact of methods such as ESOP, close interaction and collaboration is needed with experts in the epidemiological and social sciences to better align ESOP with professional epidemiological forecasting and economic forecasting models. ESOP's interaction with these models is of a *black-box* nature which makes integration smoother and simpler.

## Code Availability

All code used for this study is available at the following GitHub Repository  
<https://github.com/purushottamkar/esop>



## References

- Julia E Aledort, Nicole Lurie, Jeffrey Wasserman, and Samuel A Bozzette. Non-pharmaceutical public health interventions for pandemic influenza: an evaluation of the evidence base. *BMC Public Health*, 7(208), 2007.
- Benjamin Bolker. Chaos and complexity in measles models: A comparative numerical study. *IMA Journal of Mathematics Applied in Medicine & Biology*, 10:83–95, 1993.
- Stephen Boyd and Lieven Vandenbergh. *Convex Optimization*. Cambridge University Press, 2004.
- Raj Dandekar and George Barbastathis. Neural Network aided quarantine control model estimation of global Covid-19 spread. arXiv:2004.02752v1 [q-bio.PE], April 2020.
- Denis Efimov and Rosane Ushirobira. On an interval prediction of COVID-19 development based on a SEIR epidemic model. Technical report, Inria Lille Nord Europe - Laboratoire CRISTAL - Université de Lille, April 2020. hal-02517866v4.
- Andreas Eilersen, Mogens H. Jensen, and Kim Sneppen. Chaos in disease outbreaks among prey. *Scientific Reports*, 10(3907), 2020.
- Neil M Ferguson, Daniel Laydon, Gemma Nedjati-Gilani, Natsuko Imai, Kylie Ainslie, Marc Baguelin, Sangeeta Bhatia, Adhiratha Boonyasiri, Zulma Cucunubá, Gina Cuomo-Dannenburg, Amy Dighe, Ilaria Dorigatti, Han Fu, Katy Gaythorpe, Will Green, Arran Hamlet, Wes Hinsley, Lucy C Okell, Sabine van Elsland, Hayley Thompson, Robert Verity, Erik Volz, Haowei Wang, Yuanrong Wang, Patrick GT Walker, Caroline Walters, Peter Winskill, Charles Whittaker, Christl A Donnelly, Steven Riley, and Azra C Ghani. Impact of non-pharmaceutical interventions (NPIs) to reduce COVID-19 mortality and healthcare demand. Technical report, Imperial College London, 2020.
- Peter I. Frazier. A Tutorial on Bayesian Optimization. arXiv:1807.02811v1 [stat.ML], July 2018.
- Donald R. Jones, Matthias Schonlau, and William J. Welch. Efficient Global Optimization of Expensive Black-Box Functions. *Journal of Global Optimization*, 13:455–492, 1998.
- Matt J. Keeling and Pejman Rohani. *Modeling Infectious Diseases in Humans and Animals*. Princeton University Press, 2008.
- Ryder Kimball and Debanjali Bose. 11 pandemics that changed the course of human history, from the Black Death to HIV/AIDS - to coronavirus. Business Insider India, March 2020. <https://www.businessinsider.in/science/news/11-pandemics-that-changed-the-course-of-human-history-from-the-black-death-to-hiv/aids-to-coronavirus/articleshow/74695609.cms>. Accessed 19 April 2020.
- Tom Lindström, Michael Tildesley, and Colleen Webb. A Bayesian Ensemble Approach for Epidemiological Projections. *PLOS Computational Biology*, 11(4):e1004187, 2015.
- Wladimir Lyra, José-Dias do Nascimento Jr., Jaber Belkhiria, Leandro de Almeida, Pedro Paulo M. Chrispim, and Ion de Andrade. COVID-19 pandemics modeling with SEIR(+CAQH), social distancing, and age stratification. The effect of vertical confinement and release in Brazil. medRxiv: 2020.04.09.20060053, April 2020.
- Itamar Megiddo, Abigail R. Colson, Arindam Nandi, Susmita Chatterjee, Shankar Prinja, Ajay Khera, and Ramanan Laxminarayan. Analysis of the Universal Immunization Programme and introduction of a rotavirus vaccine in India with IndiaSim. *Vaccine*, 325:A151–A161, 2014.
- Dylan H. Morris, Fernando W. Rossine, Joshua B. Plotkin, and Simon A. Levin. Optimal, near-optimal, and robust epidemic control. arXiv:2004.02209v1 [q-bio.PE], April 2020.

- Oscar Patterson-Lomba. Optimal timing for social distancing during an epidemic. medRxiv: 2020.03.30.20048132, April 2020.
- Corey M. Peak, Lauren M. Childs, Yonatan H. Grad, and Caroline O. Buckee. Comparing nonpharmaceutical interventions for containing emerging epidemics. *Proceedings of the Nat. Acad. Sci. USA Sciences of the USA*, 114(15):4023–4028, 2017.
- Carl Edward Rasmussen and Christopher K. I. Williams. *Gaussian Processes for Machine Learning*. MIT Press, 2006.
- Robert Roos. CDC estimate of global H1N1 pandemic deaths: 284,000. Newsletter of the Center for Infectious Disease Research and Policy, University of Minnesota, June 2012. <https://www.cidrap.umn.edu/news-perspective/2012/06/cdc-estimate-global-h1n1-pandemic-deaths-284000>. Accessed 19 April 2020.
- Tridip Sardar, Sk Shahid Nadimb, and Joydev Chattopadhyay. Assessment of 21 Days Lockdown Effect in Some States and Overall India: A Predictive Mathematical Study on COVID-19 Outbreak. arXiv:2004.03487v1 [q-bio.PE], April 2020.
- Anna Scherbina. Determining the Optimal Duration of the COVID-19 Suppression Policy <https://dx.doi.org/10.2139/ssrn.3562053>. Accessed 19 April 2020., March 2020.
- Snehal Shekatkar, Bhalchandra Pujari, Mihir Arjunwadkar, Dhiraj Kumar Hazra, Pinaki Chaudhuri, Sitabhra Sinha, Gautam I Menon, Anupama Sharma, and Vishwesh Guttal. INDSCI-SIM: A state-level epidemiological model for India, 2020. Ongoing Study at <https://indscicov.in/indscisim>.
- Rajesh Singh and Ronojoy Adhikari. Age-structured impact of social distancing on the COVID-19 epidemic in India. arXiv:2003.12055v1 [q-bio.PE], March 2020.
- C. P. Vyasarayani and Anindya Chatterjee. New approximations, and policy implications, from a delayed dynamic model of a fast pandemic. arXiv:2004.03487v1 [q-bio.PE], April 2020.
- Jacco Wallinga, Michiel van Boven, and Marc Lipsitch. Optimizing infectious disease interventions during an emerging epidemic. *Proceedings of the Nat. Acad. Sci. USA Sciences of the USA*, 107(2):923–928, 2010.
- WHO. Coronavirus disease (COVID-19) Pandemic, April 2020. <https://www.who.int/emergencies/diseases/novel-coronavirus-2019>. Accessed 19 April 2020.